Determination of Luminosity With Thermal Neutron Counting Using TPX Detectors in the ATLAS Cavern in LHC Proton-Proton Collisions at 13 TeV

André Sopczak, *Senior Member, IEEE*, Babar Ali, Jakub Begera, Benedikt Bergmann, Thomas Billoud, Bartoloměj Biskup, Petr Burian, Davide Caforio, *Member, IEEE*, Erik Heijne, *Fellow, IEEE*, Josef Janeček, Claude Leroy, *Member, IEEE*, Petr Mánek, Yesid Mora, Stanislav Pospíšil, *Senior Member, IEEE*, Thomas Seidler, Michal Suk, and Zdeněk Svoboda

***Abstract*— A network of Timepix (TPX) devices installed in the ATLAS cavern has the unique capability of measuring the luminosity with thermal neutron counting in Large Hadron Collider proton-proton collisions at 13 TeV. Compared with the hit-counting method, the method of thermal neutron counting has the advantage that it is not affected by induced radioactivity. The results of the luminosity determination are presented for several independently operated TPX detectors. The long-term time stability measurements of the luminosity are presented for individual devices and between different devices. The high-statistics data sets allow a detailed comparison between neutron counting and hit-counting luminosity determinations.**

***Index Terms*— Active pixel sensors, colliding beam accelerators, Large Hadron Collider (LHC), luminosity, neutrons,**

I. Introduction

THE precision measurement of the Large Hadron Collider (LHC) luminosity is important for many physics analyses performed by the ATLAS and CMS collaborations at CERN, and thus, the luminosity measurements attract much attention. The ATLAS and CMS collaborations have elaborate systems of luminosity measurements, described in [1] and [2] (ATLAS) and [3] and [4] (CMS). In this paper, the capabilities to contribute to the overall luminosity measurements with a completely different method as studied before [5] (hit counting), namely, using thermal neutron counting, are explored. For the luminosity measurements, the long-term time stability is of particular interest. Any further information on the LHC luminosity is a valuable addition to the previously explored hit-counting luminosity [5] and would constitute an important advancement in the overall LHC luminosity determination. The neutron counting capabilities in the ATLAS cavern at CERN are unique to the TPX detector network. The network of 16 devices [6] and their locations are shown in Fig. 1.

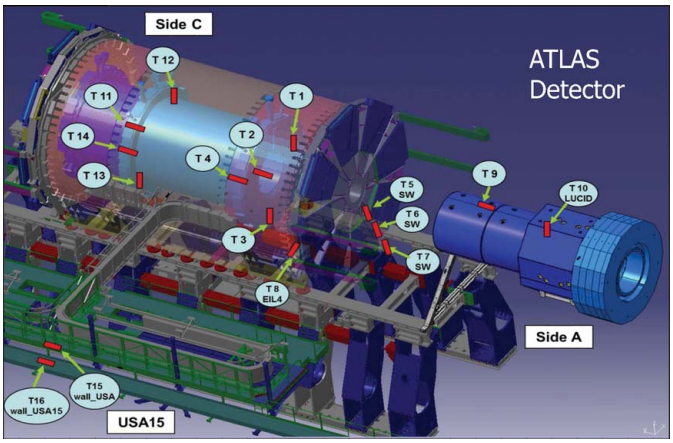

Fig. 1. Overview of TPX detector positions in the ATLAS detector (partial illustration) and in the ATLAS cavern. The devices TPX01 to TPX16 are indicated as T1 to T16.

Each TPX device consists of two stacked hybrid silicon pixel sensors. The silicon sensors consist of a matrix of 256 × 256 pixels of 55 μm pitch, and a thickness of 300 μm (further indicated as layer-1) and 500 μm (layer-2) [7]. The readout chips connected to these sensors have the original Timepix design [8], [9]. The installation of the TPX devices took place during the LHC shutdown transition from Run-1 to Run-2 in 2013/2014. These double-layer TPX devices replaced the previously operational network that employed single-layer Medipix (MPX) assemblies [10], [11].

These devices measure the primary and secondary particle fluxes resulting from 13 TeV proton-proton collisions. The data were taken in 2015 during the first year of LHC Run-2 operation.

The use of the TPX network for luminosity measurements has several advantages compared with the previous luminosity measurements [12] at LHC during Run-1 that used MPX devices. The two-layer hodoscope structure of the TPX devices

Manuscript received November 2, 2017; revised February 23, 2018; accepted March 1, 2018. Date of publication May 22, 2018; date of current version July 16, 2018. This work was supported in part by the Ministry of Education, Youth and Sports of the Czech Republic, under Project LG 15052 and Project LM 2015058, in part by the Natural Sciences and Engineering Research Council of Canada, and in part by the European Regional Development Fund-Project, Van de Graaff Accelerator–a Tunable Source of Monoenergetic Neutrons and Light Ions, under Grant CZ.02.1.01/0.0/0.0/16_013/0001785.

A. Sopczak, B. Ali, J. Begera, B. Bergmann, B. Biskup, P. Burian, D. Caforio, E. Heijne, J. Janeček, P. Mánek, Y. Mora, S. Pospíšil, T. Seidler, M. Suk, and Z. Svoboda are with the Institute of Experimental and Applied Physics, Czech Technical University in Prague, 128 00 Prague, Czech Republic (e-mail: andre.sopczak@cern.ch).

T. Billoud and C. Leroy are with the Group of Particle Physics, University of Montreal, Montréal, QC H3T 1J4T, Canada.

Color versions of one or more of the figures in this paper are available online at http://ieeexplore.ieee.org.

Digital Object Identifier 10.1109/TNS.2018.2839683

TABLE I

TPX DEVICE LOCATIONS WITH RESPECT TO THE INTERACTION POINT. Z IS THE LONGITUDINAL DISTANCE FROM THE INTERACTION POINT AND R IS THE DISTANCE FROM THE BEAM AXIS. THEIR UNCERTAINTY IS ABOUT 10 MM. THE ORDERING IN THE TABLE IS GIVEN WITH DECREASING PARTICLE FLUXES, NORMALIZED TO 100% ACQUISITION TIME. ONLY DEVICES OPERATED FOR CLUSTER COUNTING THROUGHOUT THE YEAR 2015 ARE USED FOR THE HB (THERMAL NEUTRON) ANALYSIS, AS INDICATED. *REJECTED DURING ANALYSIS BECAUSE OF A TOO SMALL COUNT RATE

Device	Z (mm)	R (mm)	TPX clusters per unit sensor area and luminosity $(\mathrm{cm}^{-2}/\mathrm{nb}^{-1})$		Used for th. neutron analysis
			Layer-1	Layer-2	
TPX01	3540	1106	68600	78700	Yes
TPX11	-3540	1116	68500	77500	Yes
TPX02	3540	1115	67900	77900	No
TPX12	-3540	1146	63800	72300	No
TPX03	3540	1140	62400	72300	Yes
TPX05	7830	1409	71.9	83.9	Yes
TPX04	2830	3709	43.6	50.6	Yes
TPX14	-2830	3709	42.4	48.7	Yes
TPX06	7830	2584	19.0	22.2	Yes
TPX07	7830	3663	7.70	9.56	Yes
TPX09	15390	1560	6.06	7.31	Yes
TPX08	7220	6140	1.76	2.12	Yes
TPX15	5020	16690	0.24	0.30	No*

doubles the measurement statistics and allows one to determine the precision and long-term time stability of individual TPX devices [5]. The dead time caused by the readout was reduced from about 6 s to 0.12 s allowing a much higher data acquisition rate. Also, the TPX devices are operated in three different modes [8], [9]: hit-counting; time-over-threshold (energy deposits and cluster-counting); and time-of-arrival (cluster-counting).

The TPX network is self-sufficient for luminosity monitoring. It collects data independently of the ATLAS data-recording chain [1], [2], and provides independent measurements of the bunch-integrated LHC luminosity. In particular, van der Meer (vdM) scans [13] can be used for an absolute luminosity calibration.

The detection of charged particles in the TPX devices is based on the ionization energy deposited by particles passing through the silicon sensor. The signals are processed and digitized during an adjustable exposure time (frame acquisition time) for each pixel. Neutral particles, namely neutrons, however, need to be converted to charged particles before they can be detected. Therefore, a part of each silicon sensor is covered by ^{6}LiF and polyethylene converters [7], [14].

Thirteen out of the sixteen installed devices have been used for the luminosity analysis. Two devices were found to be inoperational after the closing of the ATLAS detector, and one device was intentionally located far away from the interaction point, and therefore, it was unusable for luminosity measurements. Table I lists the locations of the 13 devices and their numbers of registered passing particles (clusters), normalized to 100% acquisition time. It was noted that the number of clusters for the 500 μm sensor is about 20% larger compared with that of the 300 μm sensor [5]. This

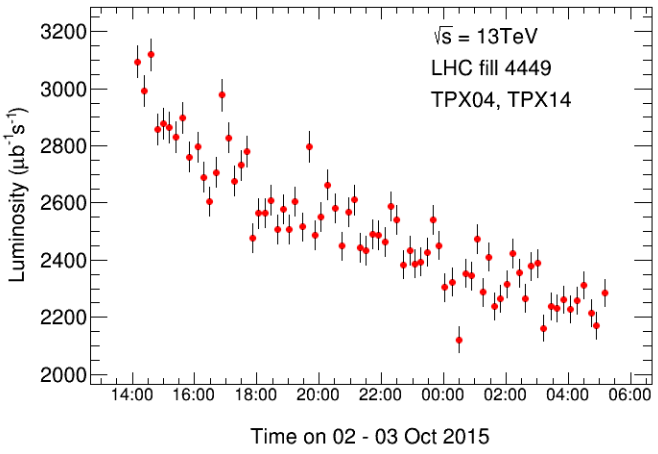

Fig. 2. Time history of the TPX luminosity using thermal neutron counting. The descending LHC luminosity curve is clearly visible. The error bars give the statistical uncertainty. The normalization between hit rate and luminosity is based on the vdM scan using the LHC fill 4266, determined with the TPX hit-counting [5], and details are given in the text and in Fig. 3. The small dip at 0:30, visible as variation from the descending curve, corresponds to the time when the LHC operators performed small-amplitude beam separation scans to optimize the luminosity.

percentage is lower than might be expected from the 40% larger sensitive volume, because the extended clusters induced by a single particle count only "one" in the thin as well as in the thick sensor. The number of photon conversions and fast neutron interactions, however, will increase with the sensitive volume. The analysis described in this paper is focused on the thermal neutron counting luminosity determination with all devices, except TPX02 and TPX12 (which were operated with 1 s exposure time at high particle fluxes, and thus, had no possibility to identify clusters) [5]. During 2015 LHC proton-proton collisions, typical luminosities at the beginning of the LHC fills were $\mathcal{L} = 3\text{–}5{\cdot}10^{33}$ cm^{-2}s^{-1} = 3000–5000 μb^{-1}s^{-1}.

Fig. 2 shows an example of the luminosity measurement from thermal neutron counting determined with the TPX devices indicated in Table I for layer-1 and layer-2 combined. The LHC fill 4449 was taken on October 2–3, 2015, and times are in GMT. The normalization between neutron count rates and luminosity is based on the vdM scan using the LHC fill 4266, determined with TPX hit-counting [5] as detailed in Section II.

This paper is structured as follows. First, the concept of LHC luminosity monitoring from TPX thermal neutron counting is introduced in Section II. The long-term luminosity precision is given in Section III from the comparison of layer-1 and layer-2 results of the same TPX device. The long-term luminosity precision from different TPX devices is given in Section IV. A comparative study of thermal neutron and hit-counting luminosity is given in Section V. Finally, conclusions are given in Section VI.

II. TPX LUMINOSITY FROM THERMAL NEUTRON COUNTING

Thermal neutrons are detected by TPX devices via ^{6}Li(n, α)^{3}H reactions in a ^{6}LiF converter layer of a

(1.6 ± 0.3) mg/cm^2 ^{6}LiF foil (^{6}Li enrichment: 89%) [7]. The tritons and alpha particles from the neutron conversion are registered by Si-sensors as large round-shaped pixel clusters, so-called heavy blobs (HBs). The typical detection efficiency for thermal neutrons is about 0.5%, determined from individual calibrations of the TPX devices in a thermal neutron field [7]. A background HB count rate resulting from charged particles with high stopping power has been subtracted based on the HB count rate in region without LiF converter. For example, TPX04 layer-1 has a 20% background rate. Hence, the background-corrected HB count rate is proportional to the number of neutrons passing the devices. It is used as a measure of instantaneous luminosity since neutrons are generated in the primary and secondary interactions from the proton-proton collisions. This method was pioneered with MPX devices for LHC Run-1 operation [15].

For the devices TPX01 to TPX15 (except for TPX02 and TPX12), the pixel matrix occupancy is sufficiently small for pattern recognition and to determine the HB (thermal neutron) count rate. This was achieved by different acquisition times of 1 ms to 1 s depending on the device. With the typical HB count rates of order one per frame, the possible misidentification of HBs, which are lost due to the overlap with other clusters [11, Sec. 2.2], is negligible.

The number of HB per frame is converted into the number of HB per luminosity block (LB) [12] of 60 s length. Frames are selected which lie within the time window of the LB, and the numbers of HB of these frames are averaged. The changes of acquisition time during the 2015 data-taking for individual devices are taken into account. TPX15 was then excluded in the analysis because of a too small count rate.

These LBs are grouped into time periods corresponding to LHC fill time periods with varying length from about 1 to 20 h (typically more than 6 h). For each LB time interval, the number of HB is summed. This summed number of HB is converted into luminosity by using a normalization factor determined from TPX hit-counting luminosity [5] based on the averaged luminosity measurement from TPX02 and TPX12, layer-1 and layer-2, respectively. Fig. 3 shows the linearity between HB counts per LB (for 100% acquisition time) and the TPX hit-counting luminosity per LB [5]. The slope of the fit corresponds to the inverse normalization factor $(1/n_{\mathrm{f}})$. The normalization factors for all TPX devices used for thermal neutron counting are summarized in Table II.

For each device and each time period, the relative statistical uncertainty is $1/\sqrt{N_{\mathrm{HB}}}$, where N_{HB} is the summed number of HBs. The statistical uncertainties are dominant in the analysis of HB counting in the ^{6}LiF-covered detector region, since the HB count rate is rather small (up to a few 100 counts per LB and device layer).

III. Long-Term Stability of Individual TPX Devices

The long-term time stability of the luminosity monitoring is determined for individual TPX devices by comparing the luminosity between the two separate sensitive layers of the TPX devices. For this analysis, the LBs are grouped corresponding to time periods of the 2015 LHC fills. A linear fit is applied to the (layer-1)/(layer-2) luminosity ratio versus time for the September to November 2015 data-taking period, as given in Fig. 4 for the examples of TPX04 and TPX14 devices, which are located at about opposite positions from the primary interaction point. The slopes of the linear fits are taken as a measure of time stability. The uncertainties on the slopes are obtained from the fits. As the statistical uncertainty of the ratio measurements for the grouped LB is much larger than possible systematic uncertainties, the fits take only the statistical uncertainties into account. The obtained slope values and their uncertainties for four TPX sensors are summarized in Table III.

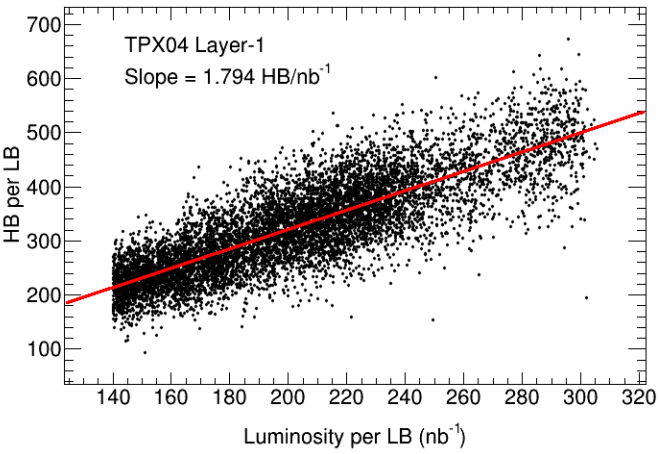

Fig. 3. Thermal neutron (HB) rate per LB (for 100% acquisition time) versus TPX hit-counting luminosity per LB [5] for TPX04 layer-1. The slope of the linear fit gives the normalization factor between count rate and thermal neutron luminosity. The scatter of the points is larger than purely statistical with $\chi^2/\mathrm{ndf} = 3.5$.

TABLE II
Inverse Normalization Factors $(1/n_{\mathrm{f}})$ to Convert HB Rates to Luminosities

Device	$1/n_{\mathrm{f}}$ (HB/nb^{-1})	
	Layer-1	Layer-2
TPX01	138.7	57.51
TPX03	142.7	101.2
TPX04	1.794	1.658
TPX05	2.357	2.987
TPX06	0.7693	0.6960
TPX07	0.1397	0.1359
TPX08	0.01446	0.01158
TPX09	0.06091	0.04994
TPX11	162.8	103.2
TPX14	1.876	1.922

TABLE III
Slope of Time History of the Luminosity Ratio Measured by Layer-1 and Layer-2 for TPX04 and TPX14. The Slope Values and the Uncertainties are Given per Second and in Percent per 100 Days

TPX	Slope (10^{-10} s^{-1})	σ_{Slope} (10^{-10} s^{-1})	Slope (%/100d)	σ_{Slope} (%/100d)
04	−4.77	8.63	−0.41	0.75
14	0.27	14.67	0.02	1.27

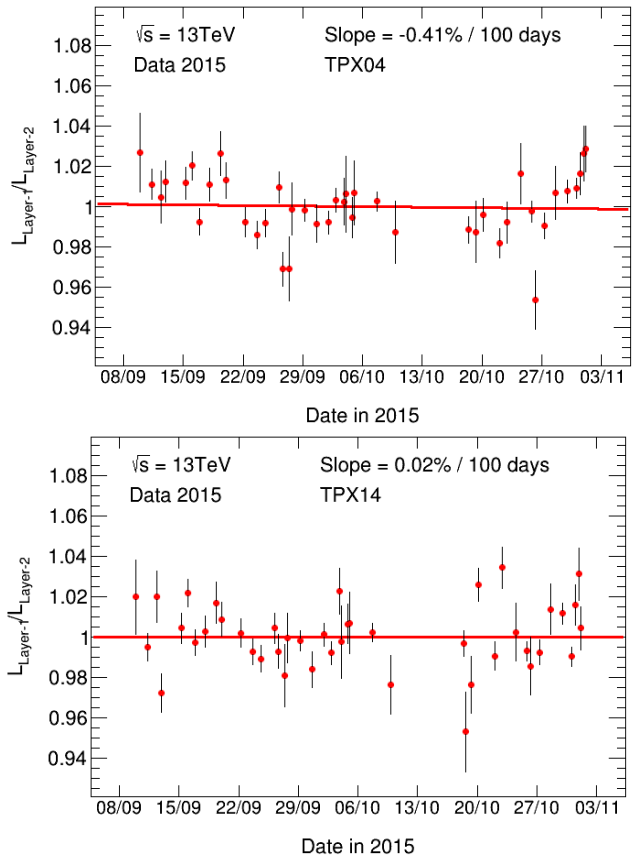

Fig. 4. Time history of the luminosity ratio measured by layer-1 and layer-2 for TPX04 and TPX14. The 2015 TPX data are divided into LBs of typically 1-min length and then grouped into LHC fill time periods. The statistical error bars are given. A linear fit is applied to determine the slope. The LHC fills from September to November 2015 are shown.

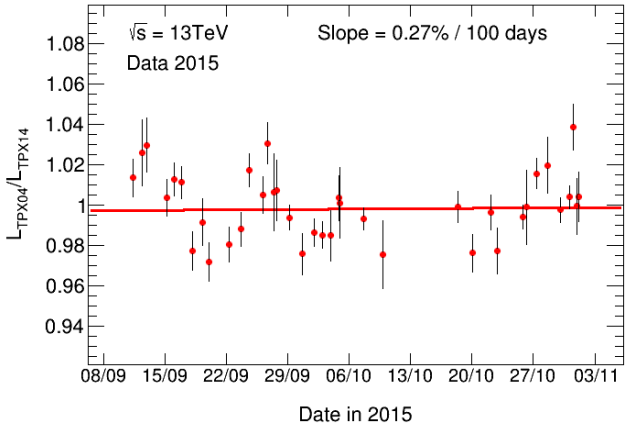

Fig. 5. Time history of the luminosity ratio measured by TPX04 and TPX14. The measurements are averaged over the data recorded by layer-1 and layer-2. The 2015 TPX data are divided into LBs of typically 1-min length and then grouped into LHC fill time periods. The statistical error bars are given. A linear fit is applied to determine the slope. The LHC fills from September to November 2015 are shown.

TABLE IV

SLOPE OF TIME HISTORY OF THE LUMINOSITY RATIO MEASURED BY TPX04 AND TPX14. THE MEASUREMENTS ARE AVERAGED OVER THE DATA RECORDED BY LAYER-1 AND LAYER-2. THE SLOPE VALUES AND THE UNCERTAINTIES ARE GIVEN PER SECOND AND IN PERCENT PER 100 DAYS

TPX	Slope ($10^{-10}\,s^{-1}$)	σ_{Slope} ($10^{-10}\,s^{-1}$)	Slope (%/100d)	σ_{Slope} (%/100d)
04/14	3.16	10.20	0.27	0.88

The slopes show that the luminosity ratio measured by layer-1 and layer-2 has no significant variation with time. This indicates no significant relative change in sensitivity with time between the thinner and thicker sensors. The long-term stability of the luminosity measurements between individual layers is below 1% per 100 days.

IV. LONG-TERM STABILITY OF DIFFERENT TPX DEVICES

The long-term time stability of the luminosity monitoring is determined for different TPX devices located up to about 7 m apart at opposite sides of the primary proton-proton interaction point. First, the frames are grouped into LBs of about 1 min. This grouping of frames is necessary for a comparative study as the start times of the frames are not synchronized between the TPX devices. Then, the LBs are grouped into time periods corresponding to the LHC fills. The luminosity ratio of TPX04 and TPX14 is calculated as the average over layer-1 and layer-2, and a linear fit is applied for the September to November 2015 data-taking period, as given in Fig. 5. The slope of the linear fit is taken as a measure of time stability. The uncertainty on the slope is obtained from the fit. As the statistical uncertainty of the ratio measurements for the grouped LB is much larger than possible systematic uncertainties, the fit takes only the statistical uncertainty into account. The obtained slope value and its uncertainty are summarized in Table IV. Some fluctuations around the slope of 0.27% per 100 days are observed. These fluctuations could either result from the TPX operation or from small variations in the complex LHC radiation field depending on small changes in the colliding beam optics. The study of the different TPX devices indicates an internal time stability of the luminosity measurement below 1% per 100 days.

V. COMPARISON OF THERMAL NEUTRON AND HIT-COUNTING LUMINOSITY MEASUREMENTS

For this study of the relative neutron luminosity precision, the TPX thermal neutron luminosity and the TPX hit-counting luminosity measurements [5] are compared fill-by-fill. The relative TPX hit-counting fill-by-fill uncertainty was 0.5% [5].

The ratio of the TPX thermal neutron luminosity measurements $L_{TPX}^{neutrons}$ and the TPX hit-counting reference luminosity L_{TPX}^{hits} [5] is shown in Fig. 6 as a function of time. The LBs in each recorded LHC fill are combined, and the statistical uncertainty on the luminosity ratio is indicated by the error bars. The LHC fills with less than 50 LBs are excluded.

The relative differences between the thermal neutron and the hit-counting luminosity measurements are approximately described by a single Gaussian fit with a width (sigma) of $(0.97 \pm 0.23)\%$ (Fig. 7). The width is dominated by the

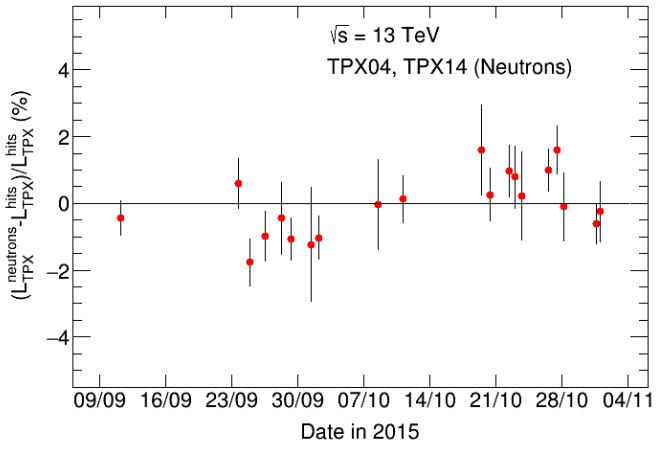

Fig. 6. Evolution in time of the fractional difference in fill-integrated luminosity between the TPX neutron-counting and the TPX hit-counting reference luminosity. Each point shows the mean difference for a single LHC fill as defined in the text. The error bars are statistical only, and convoluted with 0.5% relative uncertainty from the TPX hit-counting reference measurement. The TPX neutron luminosity is normalized to the TPX hit-counting luminosity [5]. The data of the devices TPX04 and TPX14, layer-1 and layer-2, are combined.

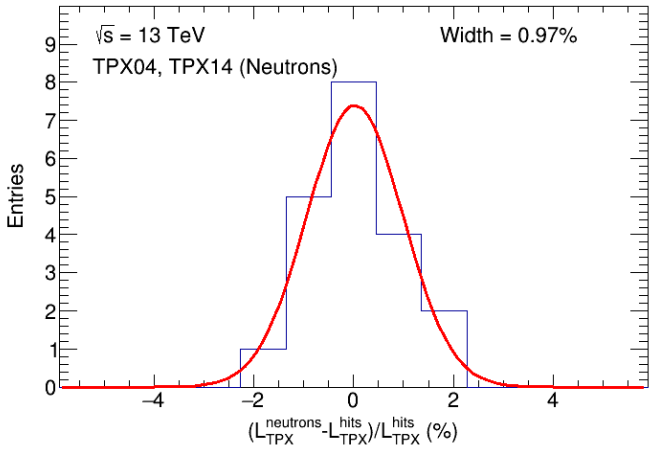

Fig. 7. Residual distributions defined as $(L_{\mathrm{TPX}}^{\mathrm{neutrons}} - L_{\mathrm{TPX}}^{\mathrm{hits}})/L_{\mathrm{TPX}}^{\mathrm{hits}}$. A Gaussian fit is applied. The TPX neutron luminosity is normalized to the TPX hit-counting luminosity [5]. The data of the devices TPX04 and TPX14, layer 1 and layer 2, are combined.

statistical uncertainty of the TPX thermal neutron measurement.

The pull distribution is shown in Fig. 8, assuming that the relative uncertainty is governed only by $1/\sqrt{N_{\mathrm{HB}}}$. The Gaussian fit of the pull distribution has a width (sigma) of 1.22 ± 0.21. This demonstrates that the uncertainty of the neutron counting luminosity is close to the statistical expectation.

The thermal neutron analysis is independent of activation effects of materials near the TPX devices. Although activation effects were observed in the TPX hit analysis from the production of light particles [12], the activation energy is too small to produce neutrons. Therefore, differently than in the hit-counting luminosity measurement [5], the uncertainty from

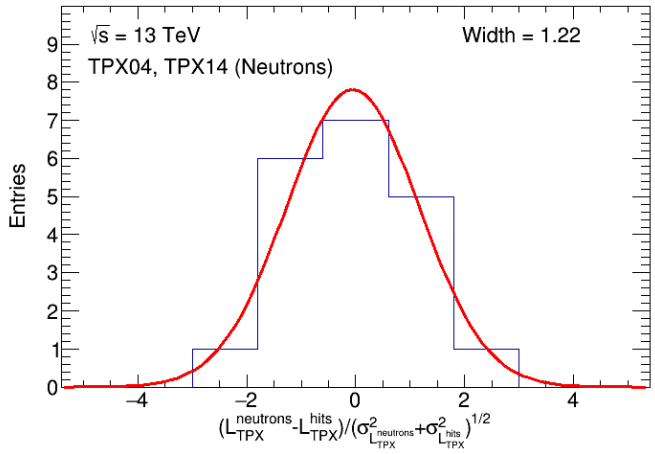

Fig. 8. Pull distribution $(L_{\mathrm{TPX}}^{\mathrm{neutrons}} - L_{\mathrm{TPX}}^{\mathrm{hits}})/(\sigma^2_{L_{\mathrm{TPX}}^{\mathrm{neutrons}}} + \sigma^2_{L_{\mathrm{TPX}}^{\mathrm{hits}}})^{1/2}$, where $\sigma_{\mathrm{L}_{\mathrm{TPX}}^{\mathrm{neutrons}}}$ is the statistical uncertainty on thermal neutron counting, and $\sigma_{\mathrm{L}_{\mathrm{TPX}}^{\mathrm{hits}}}$ the fill-by-fill uncertainty on the TPX hit-counting reference luminosity. The relative TPX hit-counting reference uncertainty is 0.5% [5]. A Gaussian fit is applied. The TPX neutron luminosity is normalized to the TPX hit-counting luminosity [5]. The data of the devices TPX04 and TPX14, layer-1 and layer-2, are combined.

the activation of detector material is absent in the present analysis.

VI. Conclusion

The network of the TPX devices installed in the ATLAS detector cavern at LHC has successfully taken data during Run-2 with 13-TeV proton-proton collisions. An independent approach to determine the LHC luminosity is presented using thermal neutron counting. The internal long-term time stability of the TPX luminosity measurements were determined for individual devices and between different devices to be below 1%. The thermal neutron luminosity measurements were compared with TPX hit-counting luminosity results. Good agreement is found within the statistical uncertainties. For an LHC fill-by-fill analysis, the relative precision is 1.0%. There is a complementarity of the thermal neutron counting and the hit-counting, and also different sets of TPX devices were used. While a hit-luminosity analysis has high statistics and its uncertainty is dominated by systematic effects, the presented thermal neutron counting analysis is dominated by statistical uncertainties owing to the limited cluster statistics. Furthermore, the neutron analysis is not affected by activation effects of material near the devices. Thermal neutron counting luminosity measurements are a valuable addition to the overall luminosity measurements.

Acknowledgment

The authors would like to thank warmly the ATLAS Luminosity Group for useful discussions and interactions and the Medipix Collaboration for providing the TPX assemblies.

References

[1] G. Aad *et al.*, "Improved luminosity determination in *pp* collisions at $\sqrt{s} = 7$ TeV using the ATLAS detector at the LHC," *Eur. Phys. J. C*, vol. 73, pp. 2518–2547, 2013.

[2] G. Aad *et al.*, "Luminosity determination in *pp* collisions at $\sqrt{s} = 8$ TeV using the ATLAS detector at the LHC," *Eur. Phys. J. C*, vol. 76, pp. 653–698, 2016.

[3] A. Ball *et al.*, "Design, implementation and first measurements with the medipix2-mxr detector at the compact muon solenoid experiment," *J. Instrum.*, vol. 6, no. 8, p. P08005, 2011.

[4] *CMS Luminosity Based on Pixel Cluster Counting—Summer 2013 Update*, document CMSPAS-LUM-13-001, CMS Public Analysis Summary CMS Collaboration, 2013.

[5] A. Sopczak *et al.*, "Precision luminosity of LHC proton–proton collisions at 13 TeV using hit counting with TPX pixel devices," *IEEE Trans. Nucl. Sci.*, vol. 64, no. 3, pp. 915–924, Mar. 2017.

[6] C. Leroy, S. Pospisil, M. Suk, and Z. Vykydal. (2014). Proposal to measure radiation field characteristics, luminosity and induced radioactivity in ATLAS with TIMEPIX devices. Project Proposal. [Online]. Available: http://cds.cern.ch/record/1646970

[7] B. Bergmann, I. Caicedo, C. Leroy, S. Pospisil, and Z. Vykydal, "ATLAS-TPX: A two-layer pixel detector setup for neutron detection and radiation field characterization," *J. Instrum.*, vol. 11, p. P10002, Oct. 2016.

[8] X. Llopart, R. Ballabriga, M. Campbell, L. Tlustos, and W. Wong, "Timepix, a 65k programmable pixel readout chip for arrival time, energy and/or photon counting measurements," *Nucl. Instrum. Methods Phys. Res. A, Accel. Spectrom. Detect. Assoc. Equip.*, vol. 581, nos. 1–2, pp. 485–494, 2007.

[9] X. Llopart, R. Ballabriga, M. Campbell, L. Tlustos, and W. Wong, "Timepix, a 65k programmable pixel readout chip for arrival time, energy and/or photon counting measurements," *Nucl. Instrum. Methods Phys. Res. A, Accel. Spectrom. Detect. Assoc. Equip.*, vol. 585, nos. 1–2, pp. 106–108, 2008.

[10] Z. Vykydal *et al.*, "The Medipix2-based network for measurement of spectral characteristics and composition of radiation in ATLAS detector," *Nucl. Instrum. Methods Phys. Res. A, Accel. Spectrom. Detect. Assoc. Equip.*, vol. 607, no. 1, pp. 35–37, 2009.

[11] M. Campbell *et al.*, "Analysis of radiation field in ATLAS using 2008–2011 data from the ATLAS-MPX network," CERN Tech. Rep. ATL-GEN-PUB-2013-001, 2013.

[12] A. Sopczak *et al.*, "MPX detectors as LHC luminosity monitor," *IEEE Trans. Nucl. Sci.*, vol. 62, no. 6, pp. 3225–3241, Dec. 2015.

[13] S. van der Meer, "Calibration of the effective beam height in the ISR," CERN Rep. ISR-PO/68-31, 1968.

[14] Z. Vykydal *et al.*, "Evaluation of the ATLAS-MPX devices for neutron field spectral composition measurement in the ATLAS experiment," in *Proc. Conf. Rec. IEEE NSS-MIC*, Oct. 2008, pp. 2353–2367.

[15] A. Sopczak *et al.*, "Luminosity from thermal neutron counting with MPX detectors and relation to ATLAS reference luminosity at $\sqrt{s} = 8$ TeV proton-proton collisions," *J. Instrum.*, vol. 12, no. 9, p. P09010, 2017.